Calculation of 3-D Magnetic Fields Produced by MHD Active Control Systems in Fusion Devices

Paolo Bettini[1,2], Lionello Marrelli[2], and Ruben Specogna[3]

[1]Università di Padova, Dipartimento di Ingegneria Industriale, Padova 35131, Italy
[2]Consorzio RFX, EURATOM-ENEA Association, Padova 35127, Italy
[3]Università di Udine, Dipartimento di Ingegneria Elettrica, Gestionale e Meccanica, Udine 33100, Italy

An accurate control of the magnetic boundary of a thermonuclear plasma is an important issue in magnetic confinement research. The development of methods for the active control of magnetohydrodynamic instabilities and correction of error fields is mandatory in view of fusion reactors or experimental test reactors under design. Recently, a very effective control scheme, named clean mode control (CMC), has been proposed in a reversed field pinch experiment (RFX-mod). The CMC is based on the real-time correction (cleaning), under simplifying hypothesis, of the sideband harmonics in the magnetic field produced by the discrete local active coils. In this paper, we focus on the problem of carefully computing the penetration of sidebands through a realistic load assembly, but still with a simplified cylindrical geometry, to allow for a detailed comparison with the crude CMC algorithm without the additional complication of the coupling between the poloidal harmonics due to the toroidal geometry.

Index Terms—**Clean mode control (CMC), MHD, periodic boundary conditions (BCs), sidebands.**

I. Introduction

An ACCURATE control of the magnetic boundary of a thermonuclear plasma is an important issue in magnetic confinement research. Close-fitting passive conducting structures are an efficient way to prevent the growth of MHD instabilities but are not suitable for a steady-state fusion reactor, because of the finite diffusion time of any material shell. Therefore, the development of methods for the active control of MHD instabilities and for the correction of error fields is mandatory in view of fusion reactors or experimental test reactors under design.

Among the major magnetic fusion concepts under consideration [1], tokamaks have been studied the most and have achieved the best overall performance, but alternative concepts are still attractive due to their physical properties or technological advantages.

In this framework, we focus on the active control of MHD instabilities in the RFX-mod experiment [2], an axisymmetric toroidal device ($R/a = 2.00/0.459$ m) characterized by 2 MA toroidal plasma current and 0.5 T toroidal flux density.

The successful simultaneous feedback control of a spectrum of MHD instabilities [both resistive wall modes (RWMs) and tearing modes (TMs) for the reversed field pinch (RFP)] allowed to reach the design plasma current of 2 MA in the RFP configuration [3]. The same feedback system has also been recently used to investigate the very low q tokamak regime, as RFX-mod can also be operated as a low current ($I_\phi = 150$ kA, $B_\phi = 0.55$ T), circular cross section, limiter tokamak. Stationary discharges with $q(a) < 2$ can be, in fact, routinely obtained because of the control of the $m = 2, n = 1$ resistive wall mode [4].

These results have been obtained because of the high degree of flexibility of the RFX-mod control system, introduced after the first phase of operation [5], which is based on a set of 48×4 saddle coils, independently driven (each saddle coil is fed with its own switching dc/dc power supply), housed inside a stainless steel toroidal support structure (Fig. 1), which surrounds a thin (3 mm) copper shell; 48×4 radial field sensor loops are located inside the shell and are processed in real time to drive currents in the control coils.

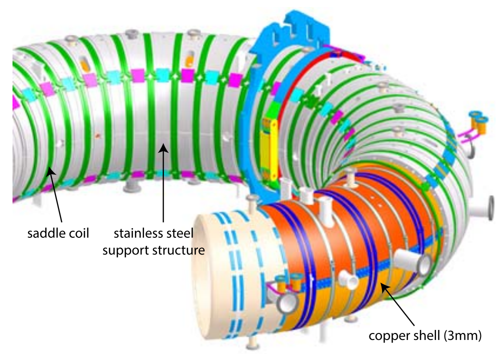

Fig. 1. Cutaway of the torus assembly of RFX-mod device. Close-fitting passive conducting structures (copper shell and stainless steel toroidal support structure) are shown, together with a subset of the 48×4 saddle coils.

RFX-mod feedback control system has been designed, in fact, to implement the intelligent shell (IS) scheme [6], in which control coils current mimic eddy currents in the shell: the control system drives currents in the control coils to cancel the measurement through a network of radial field loops of the same area. This simple control scheme allowed a significant improvement in plasma performances, compared with passive operations, by successfully stabilizing RFP RWMs [7].

Nonetheless, it was soon realized that the action of the IS control scheme on the edge value of RFP TMs was less effective due to the aliasing affecting the measured magnetic field harmonics due to high poloidal and toroidal number sidebands produced by the discrete coil grid [8]. This aliasing error has been identified and a sophisticated correction algorithm, named clean mode control (CMC), has been developed [9]. The CMC scheme is based on the real-time correction (cleaning) of the measurements from the high periodicity

Manuscript received June 28, 2013; accepted August 13, 2013. Date of current version February 21, 2014. Corresponding author: P. Bettini (e-mail: paolo.bettini@unipd.it).

Color versions of one or more of the figures in this paper are available online at http://ieeexplore.ieee.org.

Digital Object Identifier 10.1109/TMAG.2013.2279141

sidebands produced by the active coils: the feedback variables are not the raw measurements, as in the IS, but the poloidal and toroidal m, n Fourier harmonics of the radial field loops.

Because of the presence of the conducting copper shell, each sideband penetrates with different characteristic time constant and therefore pollutes the measurements in a time-dependent way. Currently, the real-time algorithm determines the sidebands subtraction in a simplified cylindrical geometry by assuming a homogeneous shell separating actuators (saddle coils) and measurements (saddle loops). Simple standard formulas for the radial magnetic field in cylindrical geometry, expressed in terms of the modified Bessel functions I_p, K_p, according to the thin-shell dispersion relation [8] are used.

The crude assumption of a single homogeneous shell cannot reproduce the irregular penetration of the radial field due to the 3-D nature of the passive structure, which are characterized by gaps and portholes. This is observed in helical boundary experiments in RFX-mod, in which the feedback law for the dominant RFP TM is modified in such a way to keep the radial field harmonic at the edge in rotation (in the range 10–40 Hz) at a finite amplitude [10]: radial and toroidal field sensors located below a region with a gap are characterized by higher amplitude oscillations and different phase delay compared with sensors located under a continuous shell. Previous attempts to compensate for these effects focused on empirically estimated modal transfer functions [10] between the actuators and the radial sensors, which did not consider the effect of the toroidal gap on the penetration of the sidebands and on the subsequent aliasing.

In this paper, we focus on the problem of carefully computing the penetration of sidebands through a realistic load assembly but still with a simplified cylindrical geometry, to allow for a detailed comparison with the crude CMC algorithm without the additional complication of the coupling between the poloidal harmonics due to the toroidal geometry. The final aim of this analysis is to quantify the effect of multiple structures and of the toroidal gaps on the aliasing of the sidebands to identify a more accurate cleaning algorithm and implement it in real time.

II. Clean Mode Control

To recall the idea behind the CMC scheme, it is convenient to refer to the single-shell configuration in cylindrical geometry (large aspect ratio approximation), which allows to investigate all the basic aspects of the problem.

A cylindrical coordinate system $(r, \theta, \phi \equiv z/R_0)$ is adopted. The plasma (minor radius $r = a$), is contained within a uniform resistive shell (minor radius $r = b$, thickness δ). The model includes a grid of $N \times M$ active coils outside the shell ($r = c$), and a grid of $N \times M$ radial field sensors inside the shell ($r = b$). Both the coils and the sensors are saddles fully covering the torus, i.e., rectangles of poloidal (azimuthal) extent $\Delta\theta = 2\pi/M$ and toroidal (longitudinal) extent $\Delta\phi = 2\pi/N$, centered at the angles $\theta_i = (i-1)\,\Delta\theta$, $i = 1, \ldots, M$, $\phi_j = (j-1)\,\Delta\phi$, $j = 1, \ldots, N$.

In this framework, a set of discrete Fourier transform (DFT) harmonics of fields $b^{m,n}_{r,\mathrm{DFT}}$ can be univocally defined in terms of radial field measurements $b^r_{i,j}$ as

$$b^{m,n}_{r,\mathrm{DFT}} = \frac{1}{\mathrm{MN}} \sum_{\substack{i=1,M\\ j=1,N}} b^r_{i,j}\, e^{-i\,(m\theta_i + n\phi_j)}. \quad (1)$$

The sampling theorem states that the DFT harmonics correspond to Fourier harmonics only if the aliasing phenomenon does not occur; i.e., if there are no Fourier harmonics beyond the spatial Nyquist spatial frequency. While this is usually true for plasma modes, the same does not hold for the infinite sequence of sideband harmonics produced by the discrete saddle coils. Therefore, each m, n DFT harmonic is the sum of all the coils sidebands, $p = m + lM$, $q = n + kN$ with $\{l, k\} \in \mathbb{Z}$

$$b^{m,n}_{r,\mathrm{DFT}} = \sum_{\substack{p=m+l\,M\\ q=n+kN\\ \{l,k\}\in\mathbb{Z}^2}} b^{p,q}_r\, f(p, q) \quad (2)$$

where the finite size of the radial field loop determines the shape factor $f(p, q)$. In the case of filamentary coils

$$f(p, q) = \sin\left(q\frac{\Delta\phi}{2}\right)\Big/\left(q\frac{\Delta\phi}{2}\right)\, \sin\left(p\frac{\Delta\theta}{2}\right)\Big/\left(p\frac{\Delta\theta}{2}\right). \quad (3)$$

Under the assumption that Fourier harmonics beyond the Nyquist limit are produced by the saddle coils only, the CMC scheme gives an estimate of the Fourier harmonic $b^{m,n}_r$ by subtracting from the DFT harmonics the contribution of the relevant sidebands as follows (notice that the m, n radial field harmonic produced by the coils is not subtracted).

$$b^{m,n}_r = \frac{1}{f(m, n)} \left[b^{m,n}_{r,\mathrm{DFT}} - \sum_{\substack{p=m+l\,M\\ q=n+kN\\ \{l,k\}\in\mathbb{Z}^2-0}} b^{p,q}_r\, f(p, q) \right]. \quad (4)$$

While this scheme is general, the present implementation [2] relies on the simplifying assumption that all the conducting structures can be modeled by a single-cylindrical thin shell without gaps and with a time constant τ_w corresponding to the sum of all the time constants of the layered structures. This means that each $p = m + lM$, $q = n + kN$ sideband, generated by a m, n current harmonic $I^{m,n}_{\mathrm{DFT}}$ penetrates the shell with a one pole transfer function

$$\frac{db^{p,q}_r}{dt} = \frac{1}{\tau^{p,q}_{\mathrm{vac}}} b^{p,q}_r + \frac{1}{\tau^{p,q}_{\mathrm{vac}}} \left(\frac{I'_p\left(\frac{qb}{R}\right)}{I'_p\left(\frac{qc}{R}\right)} L^{p,q}_c \right) I^{m,n}_{\mathrm{DFT}} \quad (5)$$

the time constant $\tau^{p,q}_{\mathrm{vac}}$ characterizes the penetration of the sideband, as a function of the effective wall time τ_w, while the $L^{p,q}_c$ constant represents the vacuum field produced by a unit coil current harmonic at the coil radius c without the presence of the shell (note that the same $f(p, q)$ factor as (3) arises because control coils have the same geometry of radial sensors)

$$\tau^{p,q}_{\mathrm{vac}} = \tau_w \frac{\left(\frac{qb}{R}\right)^2}{\left[p^2 + \left(\frac{qb}{R}\right)^2\right]} I'_p\left(n\frac{b}{R}\right) K'_p\left(q\frac{b}{R}\right) \quad (6)$$

$$L^{p,q}_c = \left(p^2 + \left(q\frac{c}{R}\right)^2\right) f^{p,q}. \quad (7)$$

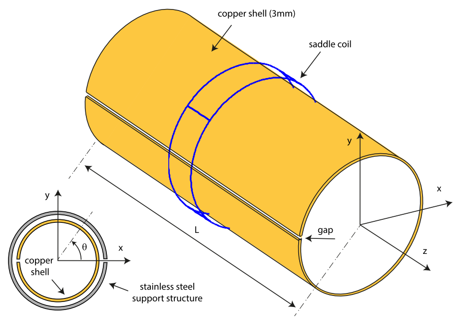

Fig. 2. Passive conductive region $\mathcal{D}_c$ includes two coaxial structures (a thin copper shell and a stainless steel structure), with continuous gaps in the longitudinal (z) direction, at $\theta = 180°$ and $\theta = 0°$, respectively. In the isometric view only the shell is shown, together with a set of four saddle coils, at the same longitudinal position.

The same procedure is performed also for the toroidal component of the field, which is used to compute the radial field in a vacuum region nearer to the plasma compared to sensors radius [8].

The aim of this paper is to lay the foundations of a more accurate cleaning procedure, by characterizing numerically the penetration of the p, q sidebands by considering the presence of a toroidal gap in a cylindrical conducting structure.

III. Discrete Geometric Formulation

A discrete geometric formulation for eddy-current problems in the frequency domain is presented, which is based on the circulation of the magnetic vector potential and exploits periodic boundary conditions (BCs) over hexahedral grids.

The 3-D domain of interest $\mathcal{D}$ is covered by a mesh of generic hexahedra, whose incidences are encoded in the cell complex $\mathcal{K}$ represented by the standard incidence matrices $\mathbf{G}$, $\mathbf{C}$, and $\mathbf{D}$ [11]. A dual barycentric complex $\tilde{\mathcal{K}}$ is obtained from $\mathcal{K}$ by the barycentric subdivision; its incidence matrices are $\tilde{\mathbf{G}} = \mathbf{D}^T$, $\tilde{\mathbf{C}} = \mathbf{C}^T$, and $\tilde{\mathbf{D}} = -\mathbf{G}^T$.

Three subdomains of $\mathcal{D}$ are identified: the passive conductive region $\mathcal{D}_c$ (including all conductive structures surrounding the plasma, see Fig. 2), the nonconductive region $\mathcal{D}_a$ (air or vacuum), and the source region $\mathcal{D}_s$ (active coils used to control the plasma instabilities).

By combining the discrete Ampère's law and Faraday's law with the discrete counterpart of the constitutive laws for the flux density $\mathbf{B}$ and the current density $\mathbf{J}$, a symmetric complex linear system of equations is obtained [12]

$$
\begin{aligned}
&(\mathbf{C}^T \boldsymbol{\nu}\, \mathbf{C})\, \mathbf{A}_r = \mathbf{0}, && \forall\ e \in \mathcal{D}_a \bigcup \mathcal{D}_s \\
&(\mathbf{C}^T \boldsymbol{\nu}\, \mathbf{C} + i\omega\boldsymbol{\sigma})\, \mathbf{A}_r = -i\omega\boldsymbol{\sigma}\, \mathbf{A}_s, && \forall\ e \in \mathcal{D}_c
\end{aligned}
\tag{8}
$$

where ω is the angular frequency, $\boldsymbol{\nu}$ and $\boldsymbol{\sigma}$ are square matrices that require metric notions, material properties, and some hypothesis on the fields to be computed.

The unknowns $\mathbf{A}_r$ are the circulations of the magnetic vector potential along primal edges $e \in \mathcal{D}$ due to eddy currents in $\mathcal{D}_c$, only. On the right-hand side (RHS), $\mathbf{A}_s$ denotes the circulations of the magnetic vector potential along $e \in \mathcal{D}_c$ produced by the sources in $\mathcal{D}_s$, only; each entry of $\mathbf{A}_s$ can be computed with standard closed formulas. Then, the circulations of the magnetic vector potential $\mathbf{A}$ can be expressed as: $\mathbf{A} = \mathbf{A}_r + \mathbf{A}_s$.

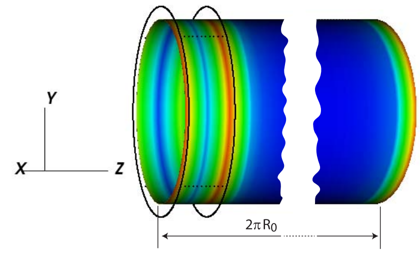

Fig. 3. Module of the current density induced on a uniform (without gap) resistive shell. Only the first four saddle coils out of 48×4 are active (fed with equal sinusoidal currents at 100 Hz).

A. Periodic Boundary Conditions

We assume a grid of $N \times M$ coils to be periodically distributed in $\mathcal{D}_s$. The numerical domain $\mathcal{D}$ is delimited by a cylindrical surface ($\mathcal{S}_1$, with minor radius $r \gg c$) and two boundary planes ($\mathcal{S}_2$, at $z = 0$ and $\mathcal{S}_3$, at $z = L = 2\pi R_0$).

The flux density distribution on $\mathcal{S}_2$ and $\mathcal{S}_3$ is identical, due to the symmetry of the conductive structures and the periodicity of the sources (it is intrinsic in toroidal devices and must be imposed in the cylindrical geometry used to derive the formulation of the CMC scheme). Since the hexahedral mesh is constructed by the sweeping of a 2-D fine quadrilateral mesh, the same degrees of freedom $\mathbf{A}_r$ are imposed on the corresponding edges $e_h \in \mathcal{S}_2$ and $e_k \in \mathcal{S}_3$, obtained by the sweeping of the same edge of the 2-D mesh. The BCs are completed by imposing $\mathbf{A}_r = 0$ on each edge of $\mathcal{S}_1$.

As a preliminary test, a set of four saddle coils (at the same longitudinal position, fed with sinusoidal currents at 100 Hz, with the same amplitude and phase) are placed around a uniform resistive thin shell. From a qualitative point of view, the correctness of the implementation is confirmed by the symmetry of the eddy currents on $\mathcal{S}_2$ and $\mathcal{S}_3$, at the opposite sides of the cylinder, as shown in Fig. 3; even though not inferable from the color scale, the values of the current densities induced on opposite sides are in an excellent agreement with respect to a 2-D axisymmetric simulation.

IV. Numerical Results

The proposed approach has been applied to the calculation of the magnetic field produced by 48×4 saddle coils, fed by sinusoidal currents ($f = 20$ Hz), in the presence of two coaxial conductive structures (a thin copper shell and a stainless steel structure), as shown in Fig. 2. To highlight the effects of the toroidal gaps, the same mesh (1 371 552 hexahedra in total; conductive structures discretized in 471 744 elements) is used for simulations both with and without gaps, by modifying accordingly the conductivity of the gap regions.

The numerical solution of the problem using computer-aided fusion engineering code,[1] takes less than 20 min, including preprocessing (assembling of the system matrix and its RHS) and post-processing (calculation of the magnetic field components by Biot-Savart's law on a fine grid of 480×140 virtual sensors).

[1] Computer-Aided Fusion Engineering (CAFE), research code developed by the authors, runs on a workstation equipped with two eight-core processors (Xeon E5-2680 2.7G Hz 20 MB) and 256 GB DDR3-1600 RAM.

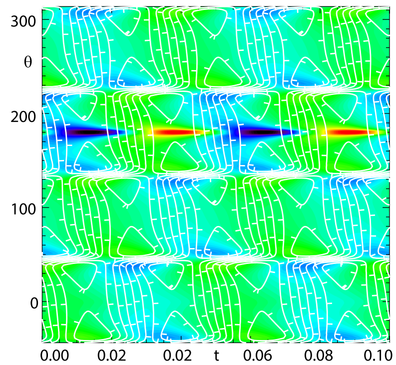

Fig. 4. Radial field calculated for different poloidal angles (θ), as a function of time. The effect of the shell's gap at $\theta = 180°$ is visible. Color map: red (+ inward), dark blue (− outward). White lines: radial field at $f = 0$ Hz.

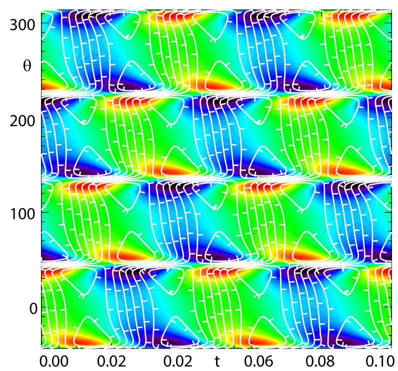

Fig. 5. Radial field calculated for different poloidal angles (θ), as a function of time. The expected pattern, without gaps, is visible. Color map: red (+ inward), dark blue (− outward). White lines: radial field at $f = 0$ Hz.

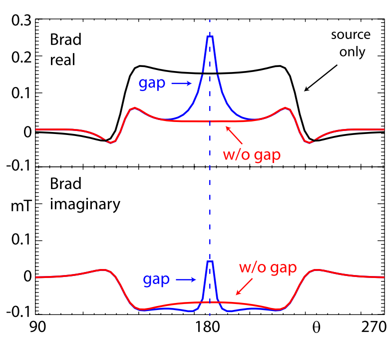

Fig. 6. Radial field as a function of the poloidal angle. The effect of the shell's gap at $\theta = 180°$ is visible.

The pattern of the radial field along the poloidal angle is shown in Figs. 4 (gaps) and 5 (w/o gaps). The effect of the shell gap is clearly visible. Then, a comparison between the radial and poloidal field components with and without gaps are shown in Figs. 6 and 7, respectively. The effects of the shell gap are clearly visible for both components.

V. Conclusion

The development of methods for the active control of MHD instabilities and for the correction of error fields is mandatory in view of fusion reactors. A very effective control scheme, named CMC, has been proposed in the RFX-mod experiment. Here, the foundations of a more accurate cleaning procedure

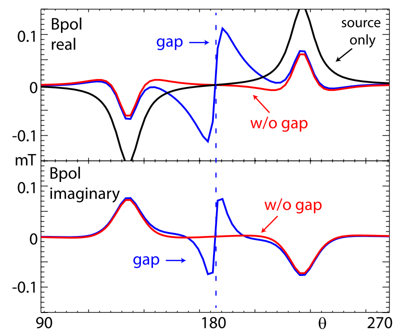

Fig. 7. Poloidal field as a function of the poloidal angle. The effect of the shell's gap at $\theta = 180°$ is visible.

have been presented, in terms of a discrete geometric formulation for eddy-current problems in the frequency domain, used to calculate the penetration of high-order sidebands in coaxial cylindrical conductive structures, by considering the presence of toroidal gaps.

Acknowledgment

This work was partially supported by the European Communities under the Contract of Association between EURATOM and ENEA/Consorzio RFX, and by the Italian MIUR under PRIN Grant 2010SPS9B3. The views and opinions expressed herein do not necessarily reflect those of the European Commission.

References

[1] J. P. Freidberg, *Plasma Physics and Fusion Energy*. Cambridge, U.K.: Cambridge Univ. Press, 2007.

[2] P. Martin, S. Martini, V. Antonia, L. Apolloni, M. Bagatina, W. Baker, *et al.*, "New insights into MHD dynamics of magnetically confined plasmas from experiments in RFX," *Nucl. Fusion*, vol. 42, no. 3, pp. 247–257, 2002.

[3] P. Martin, J. Adamek, P. Agostinetti, M. Agostini, A. Alfier, C. Angioni, *et al.*, "Overview of the RFX fusion science program," *Nucl. Fusion*, vol. 51, no. 9, pp. 094023-1–094023-12, 2011.

[4] P. Zanca, G. Marchiori, L. Marrelli, L. Piron, and the RFX-mod Team, "Advanced feedback control of magnetohydrodynamic instabilities: Comparison of compensation techniques for radial sensors, *Plasma Phys. Controlled Fusion*, vol. 54, no. 12, pp. 124018–124027, 2012.

[5] R. Piovan, F. Gnesotto, S. Ortolani, W. Baker, O. Barana, P. Bettini, *et al.* "RFX machine and power supply improvements for RFP advanced studies," *Fusion Eng. Des.*, vols. 56–57, pp. 819–824, Oct. 2001.

[6] C. M. Bishop, "An intelligent shell for the toroidal pinch," *Plasma Phys. Controlled Fusion*, vol. 31, no. 7, pp. 1179–1189, 1989.

[7] S. Ortolani, "Active MHD control experiments in RFX-mod," *Plasma Phys. Controlled Fusion*, vol. 48, pp. B371–B381, Nov. 2006.

[8] P. Zanca, L. Marrelli, G. Manduchi, and G. Marchiori, "Beyond the intelligent shell concept: The clean-mode-control," *Nucl. Fusion*, vol. 47, no. 11, pp. 1425–1436, 2007.

[9] L. Marrelli, P. Zanca, M. Valisa, G. Marchiori, A. Alfier, F. Bonomo, *et al*, "Magnetic self organization, MHD active control and confinement in RFX-mod," *Plasma Phys. Control. Fusion*, vol. 49, pp. B359–B369, Nov. 2007.

[10] L. Piron, J. M. Hanson, Y. In, G. Marchiori, L. Marrelli, P. Martin, *et al*, "Improved dynamic response of magnetic feedback in RFX-mod and DIII-D," *Plasma Phys. Controlled Fusion*, vol. 53, no. 8, pp. 084004-1–084004-14, 2011.

[11] E. Tonti, *The Mathematical Structure of Classical and Relativistic Physics*. Basel, Switzerland: Birkhäuser, 2013.

[12] A. Pirani, M. Ricci, R. Specogna, A. Tamburrino, and F. Trevisan, "Multi-frequency identification of defects in conducting media," *Inverse Problems*, vol. 24, no. 3, pp. 035011-1–035011-18, 2008.